Original article

In-vitro and computational analysis of Urolithin-A for anti-inflammatory activity on Cyclooxygenase 2 (COX-2)

Archana G. Revankar [a], Zabin K. Bagewadi [a,*], Ibrahim Ahmed Shaikh [b], Basheerahmed Abdulaziz Mannasaheb [c], Mohammed M. Ghoneim [c], Aejaz Abdullatif Khan [d], Syed Mohammed Basheeruddin Asdaq [c]

[a] Department of Biotechnology, KLE Technological University, Hubballi, Karnataka 580031, India
[b] Department of Pharmacology, College of Pharmacy, Najran University, Najran 66462, Saudi Arabia
[c] Department of Pharmacy Practice, College of Pharmacy, AlMaarefa University, Ad Diriyah 13713, Saudi Arabia
[d] Department of General Science, Ibn Sina National College for Medical Studies, Jeddah 21418, Saudi Arabia

ARTICLE INFO

ABSTRACT

Cyclooxygenase 2 (COX-2) participates in the inflammation process by converting arachidonic acid into prostaglandin G2 which increases inflammation, pain and fever. COX-2 has an active site and a heme pocket and blocking these sites stops the inflammation. Urolithin A is metabolite of ellagitannin produced from humans and animals gut microbes. In the current study, Urolithin A showed good pharmacokinetic properties. Molecular docking of the complex of Urolithin A and COX-2 revealed the ligand affinity of -7.97 kcal/mol with the ligand binding sites at TYR355, PHE518, ILE517 and GLN192 with the 4-H bonds at a distance of 2.8 Å, 2.3 Å, 2.5 Å and 1.9 Å. The RMSD plot for Urolithin A and COX-2 complex was observed to be constant throughout the duration of dynamics. A total of 3 pair of hydrogen bonds was largely observed on average of 3 simulation positions for dynamics duration of 500 ns. The MMPBSA analysis showed that active site amino acids had a binding energy of -22.0368 kJ/mol indicating that throughout the simulation the protein of target was bounded by Urolithin A. In-silico results were validated by biological assays. Urolithin A strongly revealed to exhibit anti-inflammatory effect on COX-2 with an IC_{50} value of 44.04 µg/mL. The anti-inflammatory capability was also depicted through reduction of protein denaturation that showed 37.6 ± 0.1 % and 43.2 ± 0.07 % reduction of protein denaturation for BSA and egg albumin respectively at 500 µg/mL. The present study, suggests Urolithin A to be an effective anti-inflammatory compound for therapeutic use.

* Corresponding author at: Department of Biotechnology, KLE Technological University, Vidyanagar, Hubballi 580 031, India.
E-mail addresses: 01fe21rbt001@kletech.ac.in (A.G. Revankar), zabin@kletech.ac.in (Z.K. Bagewadi), iashikh@nu.edu.sa (I.A. Shaikh), bmannasaheb@mcst.edu.sa (B.A. Mannasaheb), mghoneim@mcst.edu.sa (M.M. Ghoneim), aejaz@ibnsina.edu.sa (A.A. Khan), sasdag@mcst.edu.sa (S.M.B. Asdaq).

1. Introduction

Currently, drug designing has attained a new scenario where a comprehensive study of the molecular mechanism is being done using computation. One such is In-silico approach where, molecular docking and dynamic simulations are done to design probable pilot molecules against a specified drug target. The study output is employed to estimate the ligand's affinity for the target macromolecule by noticing the hydrophobic and ionic interactions under simulated conditions that mimic the body's environment. Cyclooxygenase (COX) is also called Prostaglandin endo-peroxide H synthases −1 and 2 (PGHS-1 and PGHS-2; also COX-1 and COX-2) (Smith et al., 2000). COX enzyme converts the Arachidonic Acid (AA) by cyclization and oxygenation into Prostaglandin G2 (PGG2) (Taidi et al., 2022; Hermanson et al., 2014). The prostaglandin synthesis by COX-2 paves the way for the progression of

numerous inflammatory conditions.COX-1 and COX-2 are two distinct isoforms within the COX enzyme family. Prostaglandin and thromboxane are made by COX-1 in a variety of cell types, including blood platelets and digestive tract cells. On the other hand, COX-2 is present during inflammatory reactions, the experience of pain, fever, and certain malignancies (Smith et al., 2000; Taidi et al., 2022). In 1977, from the sheep vesicular glands COX-1 enzyme was isolated, and it was discovered to be haem protein of 70 kDa. This particular COX variant was sequenced and the full-length cDNA corresponded to a 2.8 kb of mRNA encoding a protein of 600 amino acids. A new 4.0 kb mRNA species encoding the 600 amino acid COX-2 was discovered between 1989 and 1991 by three different groups using various experimental techniques. The initial demonstration of functional human COX-2 activity was performed in 1992 by utilizing human endothelial cells that were induced by IL-1 (Mitchell and Kirkby, 2019).The key disparity between both isoforms is that COX-1 possesses isoleucine 523 and restored by valine 523 in COX-2, results in development of a lateral hydrophobic pocket. This change subsequently induces the selectivity of inhibitors for COX-2(Taidi et al., 2022). The active site of COX-2 is notably larger by around 25% compared to that of COX-1. This structural difference grants COX-2 the capability to effectively oxygenate substrates that COX-1 either handles inadequately or not at all. This structural divergence between COX-1 and COX-2 contributes to the functional diversity observed in their respective enzymatic activities and substrate preferences (Rouzer and Marnett, 2020). The prostate, endothelium, brain and renal medulla are just a few of the organs that contain the enzyme COX-2, which can be activated. COX-1 inhibition is associated with gastrointestinal side effects and efforts to inhibit this class COX enzyme led to development of "coxibs" also called selective COX-2 inhibitors, intended to block the action of COX-2 and sparingly COX-1 at therapeutic doses (Brune and Patrignani, 2015). COX-2 possesses the capability to oxygenate the endocannabinoids N-arachidonoylethanolamine (AEA) and 2-arachidonoyiglycerol (2-AG). These endocannabinoids elicit analgesic, anti-inflammatory, and potentially anxiolytic effects by interacting with cannabinoid receptors or engaging in direct interactions with ion channels implicated in pain perception. This oxygenation by COX-2 constitutes one of the metabolic processes that terminate the biological impact of AEA and 2-AG. Certain degradation products of these endocannabinoids, such as prostamides, might serve as proinflammatory mediators (Grosser et al., 2017). NSAIDs are therapeutic agents that are widely used for pain and inflammation and the COX enzyme is the main target of this class of drugs (Baek et al., 2021). The use of NSAIDs has been observed to have caused life-threatening side effects like gastrointestinal ulceration, bleeding and perforation (Williams et al., 1999). In a prior study it is reported that co-administration of COX-2 inhibitors with compounds exhibiting analogous anti-inflammatory property is a viable method to effectively minimize NSAIDs related side effects (Kondreddy and Kamatham, 2016). This enforced the research on COX-2 active sites to design new selective Anti-inflammatory drugs (Taidi et al., 2022; Elhenawy et al., 2019).

COX −2 are target interest of NSAIDs, like aspirin, celecoxib, ibuprofen, and other new COX-2 inhibitors. These NSAIDs intensely reduce inflammation and pain, but with long-term use affects thrombotic activities and leads to cancer development (Smith et al., 2000). Fruits such as Pomegranates, blackberries, raspberries and walnuts possess a natural antioxidant Ellagitannins. Ellagitannins have been evidenced to show antioxidant, anti-inflammatory, antiviral, antimicrobial and anti-cancer effects. Urolithins are small metabolites of ellagic acid derivatives and polyphenol ellagic acid that are generated by human and animal intestinal microbiota by consumption of Pomegranate having a dibenzo alpha pyrone scaffold differently hydroxylated. Urolithins possess the inherent ability to undergo natural conjugation with methyl and glucuronide groups, leading to their distribution across various organs, plasma, urine and feces. These metabolites persist in plasma and urine for upto 72 h. As a result of their recycling within the enterohepatic system and sluggish microbial biotransformation in the colon, Urolithins exhibit elevated plasma concentrations and greater biological activity compared to their parent compounds (Ishimoto et al., 2011; Shahraki and Ebrahimi, 2019; Hasheminezhad et al., 2022).

In reported studies, Novel human gut microbiota strains that have the capability of transforming Ellagic acid (EA) to Urolithins are isolated. The identified strains are *Gordonibacterurolithinfaciens* sp. and *Ellagibacterisourolithinifaciens* (García-Villalba et al., 2022). Strains such as *Bifidobacterium pseudocatemulatun* INIA P815 was found to produce Urolithin A and Urolithin B (Gaya et al., 2018). *Lactococcus garvieae* FUA009 a gut bacterium is capable of converting ellagic acid into Urolithin A under anaerobic fermentation conditions (Mi et al., 2022).Urolithins have shown to have prominent health benefits associated with diet and biological activities like cardioprotective, antidiabetic, anti-cancer, anti-inflammatory, anti-oxidant, neuroprotective and nephroprotective (Dellafiora et al., 2020; Jing et al., 2019). Urolithins A and B are the major metabolites formed according to metabolism studies (Noshadi et al., 2020). The current study is performed based on the anti-inflammatory activities of Urolithin from prior research.

A study has reported that both of the compounds, Urolithin-A (Uro A) as well as Urolithin–B(Uro B) have shown significant activity by inhibiting PGE2 production after IL-1β stimulation. Furthermore, Uro-A downregulated the COX-2 and PGE-1 synthase mRNA and microsomal protein levels, claiming that Uro-A is the key compound at the source of pomegranate's anti-inflammatory property (González-Sarrías et al., 2010). A study have described through their research that Urolithin A inhibited the synthesis of Prostaglandin E2 thus reducing inflammation and also attenuated oxidative stress which is a stimulator of ERK1/2 (Nascimento et al., 2016). A reported study stated that polyphenols like punicalin, punicalagin and major metabolite Urolithin A have exhibited the significant potential to block the S-glycoprotein of SARS-CoV-2 with ACE2 receptor on host cells, through *In-silico* studies Urolithin A has shown its activity with binding energy of −6.86 kcal/mol (Suručić et al., 2021).

In current study, an *In-silico* method is employed for knowing molecular level of binding between COX-2 and Urolithin A, the study is performed according to the steps of protein preparation wherein 3D structure of human COX-2 is retrived from RCSB database, ligand selection is done by submitting SMILES of Urolithin A to PASS server website to predict presence of anti-inflammatory property, pharmacokinetic studies is done by Lipinski,s rule of five and ADMET studies, molecular docking of Uro A into the binding site of COX-2 is studied by utilizingAutoDock software. The docking process includes processing of protein, docking with the ligand, grid box generation and analysis of docking for best docking score pose of ligand and protein.

Molecular dynamics and simulations is done for determining stability between Urolithin and COX-2 in defined environmental conditions. The Gromacs package is used for Molecular dynamics and simulations to investigate Root-Mean-Square Deviation (RMSD), Root −Mean-Square Fluctuation (RMSF), Radius of gyration (Rg), solvent-accessible surface area (SASA) and Hydrogen bond interactions. Moreover, Molecular Mechanics Poison Boltzmann Surface Area Analysis (MMPBSA) is implemented to determine the protein's binding energy, and g_mmpbsa is utilized to track the binding energy of Urolithin A throughout the simulation timeframe.

The *In-silico* data is further validated through biological assays such as, *In-vitro* COX-2 assay and reduction of protein denaturation

of B.S.A and egg albumin for the anti-inflammatory potential of Urolithin A.

In-silico and *In-vitro* anti-inflammatory study were conducted using COX-2 protein due to its central role in the inflammatory response. COX-2 is an enzyme responsible for synthesizing prostaglandins, which are key molecules in inflammation, pain and fever pathways. As COX-2 is selectively induced during inflammation, targeting it allows in assessing the potential of Urolithin A to modulate the inflammatory process. By studying COX-2 inhibition using in-silico simulations and in-vitro, insight into the mechanism underlying anti-inflammatory effect of Urolithin A can be gained. Research on COX-2 enables researchers to comprehend how understudied compounds might affect inflammation and direct in the development of potential therapeutic interventions.

Not many reports are available on the current study that reports the computational and *In-silico* approach employed for getting an insight on the molecular aspects of anti-inflammatory activity on COX-2 and this provides as novelty in scientific field of knowledge.

2. Materials and methods

2.1. Protein structure and preparation

The 3D arrangement of human COX-2 protein of 2.70 Å resolution is obtained from the RCSB database (https://www.rcsb.org/) (PDB ID: 5KIR) in pdb format and is used to perform molecular docking to know the means of interaction of target ligand with it (Taidi et al., 2022; Smith et al., 2000). The 3-D Structure of Human COX-2 is visualized using Pymol software (Version 2.3). The macromolecular assembly structure is made up of two polypeptide chains (A and B), each chain comprisinga seriesof 551 amino acids (Shah et al., 2019). The 3D conformation of the human COX-2 protein chosen in the study is provided in Fig. 1. Chain A underwent *In-silico* protein preparation, involving the pre-processing of structures to establish bond orders, assign bonds, insert hydrogen atoms, and extract water molecules. The Protein Preparation Wizard (PPW) fromSchrodinger software is utilized for this purpose (Lokhande et al., 2022).

2.2. Ligands selection and its preparation

2D and 3D chemical structures of few COX-2 inhibitors are depicted in Table 1. The Molecular 2D structures were constructed with the help ofChemdraw Software (Version 12.0.1). 3D structures were constructed using Avagadro software (Version 1.2.0)
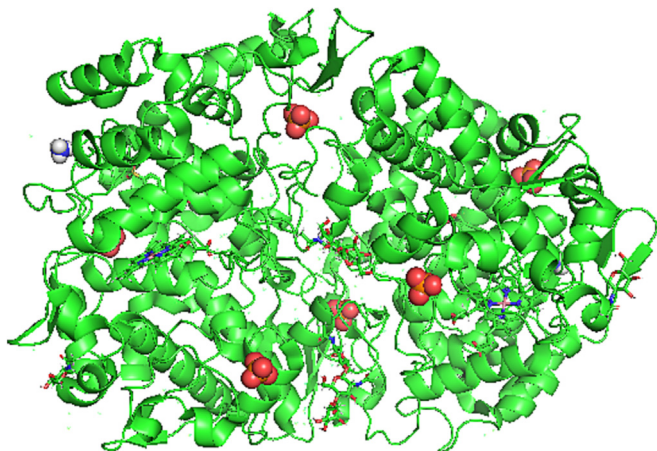

Fig. 1. 3D Structure of human Cyclooxygenase −2 protein.

and images were depicted using Discovery studio software (Version 21.1.0.20298).

From the literature survey, it is known that Urolithin A (Uro A) shows Anti-inflammatory activity. The canonical smiles of Uro A retrieved from the PubChem database (https://pubchem.ncbi.nlm.nih.gov/) are uploaded in PASS server website (https://way2-drug.com/passonline/), the word PASS here refers to Prediction of Activity Spectra for Substances. The specified tool makes use of the structural formula of a substance to anticipate a diverse range of biochemical mechanisms and pharmacological effects, facilitating the discovery of novel ligand targets and reciprocal relationships.

Biological activity spectrum concept is used wherein a list of activity names reflecting the result of interaction of chemical substance with various biological entities is done. Prediction results window shows various descriptors that are completely new, and are compared with descriptors of substances from PASS training set and interpreted. This software provides the Pa and Pi values of Uro A for Anti-inflammatory activity (Lagunin et al., 2000). The Pa refers to pharmacologically active and Pi value as pharmacologically inactive. The Canonical smiles of Uro A are submitted to the Corina Demo website (https://demos.mn-am.com/corina.html) which provided the Uro A structure in.pdb file form. The.pdb form of Uro A is downloaded and used for visualization and Molecular Docking.

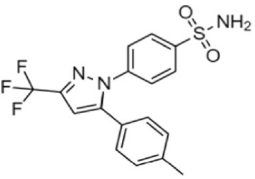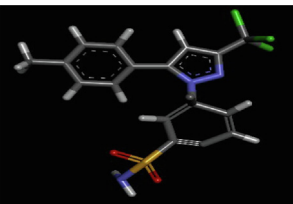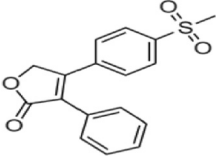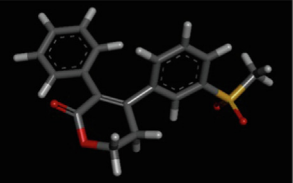### 2.3. Pharmacokinetic property studies

In a living organism, the molecule's pharmacokinetics and pharmacodynamics behaviour are influenced by several properties like hydrophobicity and molecular size. Lipinski's principles outlines the physiochemical characteristics that play a crucial role in a drug's pharmacokinetic behaviour inside human system, encompassing Absorption, Distribution, Metabolism and Excretion (ADME) (Taidi et al., 2022). To assess the ADME properties of the ligand of interest, the Canonical SMILES of Urolithin A from the PubChem webpage (https://pubchem.ncbi.nlm.nih.gov/) were provided to the Swiss ADME website (https://www.swissadme.ch/) and in preADMET Tool (https://preadmet.webservice.bmdrc.org/) (Lokhande et al., 2023).

The structure was drawn with the help of tool and the characteristics needed to fulfil as drug molecule were observed then the results are downloaded in form of an excel sheet from SwissADME and.pdb form from preADMET tool. For a Ligand to be recognized as a drug candida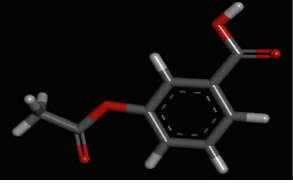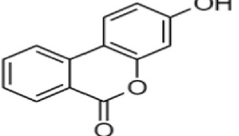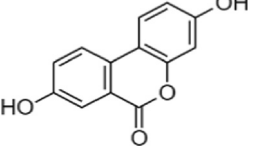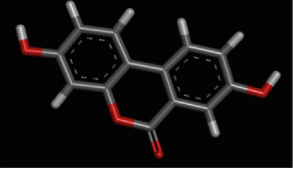te, it must satisfy the subsequent conditions: Hydrogen Bond Donor (HBD) $\leq$ 5 (OH and NH groups), Hydrogen Bond Acceptor (HBA) $\leq$ 10 (N and O atoms), partition coefficient (Clogp) $\leq$ 5,Molecular weight (MW) $\leq$ 500 g/mol and Number of rotatable bonds (nRotb) $\leq$ 10 (Taidi et al., 2022; Rasheed et al., 2018).

2.4. Molecular docking study

Pymol Visualization software is used to identify the binding domain of ligand in human COX-2 protein with ligand, along with its literature survey for prominent active sites for COX-2 used from an earlier report of (das Chagas Andrade and Mendes, 2020). The process of molecular docking is executed through the utilization of the AutoDock software (autodock suite-4.2.6-×86_64 linux3.tar) in the Ubuntu system, facilitating a cohesive environment for the docking procedure. Autodock, a proficient web based application, specializes in performing computational screening of ligands to the target of interest protein (das Chagas Andrade and Mendes, 2020).The COX-2 protein is pre-processed by selecting, choosing and preparing chain A of COX-2 by removing the ligands attached to the protein, along with eliminating water molecules and incor-

Table 1
Molecular 2D and 3D structure of Celecoxib, Rofecoxib, Diclofenac, Aspirin, Urolithin B and Urolithin A along with its IC_{50} values from earlier reports.

COX-2 inhibitor	2D Molecular Structure	3D Molecular structure	IC_{50} value	Specific COX enzyme	Reference
Celecoxib			73.53 nM	COX-2	Ahmed et al., 2020
Rofecoxib			26 ± 10 nM	COX-2	Chan et al., 1999
Diclofenac			0.84 µM	COX-2	Labib et al., 2018
Aspirin			29.3 µM	COX-2	Blanco et al., 1999
Urolithin B			>50 µM	COX-2	Noshadi et al., 2020
Urolithin A			>50 µM	COX-2	Noshadi et al., 2020
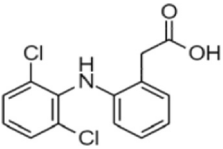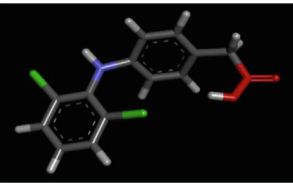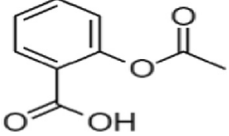
porating hydrophilic hydrogensat the binding pocket through the Autodock software (Shah et al., 2019;Taidi et al., 2022;das Chagas Andrade and Mendes, 2020). The preprocessed COX-2 protein and Uro A ligand are loaded in Autodock software.

The process of grid box formation is a pivotal step in the molecular docking procedure. It entails establishing a virtual spatial enclosure that encapsulates the active sites of the target receptor, in this case, COX-2. To achieve this, the specific x, y, z coordinates are strategically employed, delineating the exact region where the interactions between the ligand and the receptor are anticipated to occur. Notably, this step involves a meticulous selection of amino acid residues that are recognized to play an active role in the binding of the ligand, Urolithin A, with the COX-2 protein.

Among these key amino acid residues are HIS90, THR94, ARG120, GLN192, VAL349, LEU352, LEU531, SER353, LEU359, ARG513, ILE517, PHE518, VAL523, ALA527 and SER530. These residues have been carefully chosen due to their documented involvement in the binding interactions that contribute to the formation of the COX-2 and Urolithin A complex. Their strategic positioning

within the binding pocket ensures that they make crucial contacts with the ligand, anchoring and stabilizing the binding complex. Moreover these binding site residues were verified through an extensive literature survey (Shah et al., 2019;Taidi et al., 2022; More-Adate et al., 2022).

The docking was performed for the Urolithin A ligand by setting several parameters. For the generation of both grids and docking parameter files, the Autodock Tools (ADT) package is used, which includes the gridparameter files(gpf) and docking parameter file (dpf) (Taidi et al., 2022). Within the realm of molecular docking using Autodock, a pivotal parameter that assumes significance is the Lamarckian Genetic Algorithm (LGA). This algorithm imparts a distinctive approach, creating the exploration of a diverse array of possible ligand conformations, while concurrently delving into the intricacies of their local conformational space.Discovering local minima for individual conformational search is done by "Lamarckian" aspect (Shah et al., 2019; Morris and Lim-Wilby, 2008).

The results obtained from several docking simulations are automatically evaluated, leading to the creation of a Hierarchical list of

the top 10 docked conformations for Urolithin A. This list is then exported in dlg format to facilitate additional analysis (Taidi et al., 2022). The best docking score pose for the protein target is considered as good binding architecture and this result is preferred for further Molecular Dynamics and Simulations study (Dellafiora et al., 2020). After docking, the best-scored docking pose is visualized in Pymol Software to determine the interacting residues like hydrogen bonds between protein and ligand.

2.5. Molecular dynamics and simulations study

The complex of Urolithin A and COX-2 with the best docking score is chosen for Molecular Dynamics (Yaraguppi et al., 2021). MD Simulations are done using GROMACS software (2019.4) to determine the stability of Urolithin A with respect to human COX-2 protein (Taidi et al., 2022). In the study a force field of Gomocs54a7 and SPC water model is used. A prodrug server is used to obtain Ligand topology. The MD simulations are scheduled to run for 500 ns, maintaining a consistent temperature of 300 Kelvin with the help of the Berendsen thermostat. Additionally, the simulations are performed under a constant pressure of 1.01325 bars, which mirrors the physiological temperature and pressure within the human system (Yaraguppi et al., 2021; Lokhande et al., 2023).

In the tool, the complex is imported and protein preparation is compassed to observe and fix errors. In the system 10,467 explicit solvents are used to solvate the system and 38 Na$^+$ and 36 Cl$^-$ counter ions are used to neutralize the system by the steepest descent method the system is energy minimized throughout the 500 ns MD simulations (Yaraguppi et al., 2022; Lokhande et al., 2021; Lokhande et al., 2022). Input file name, grid maps coherent format and non-standard atom existence were evaluated to validate the MD simulations (Shah et al., 2019). Gromacs Package is used to analyse the data obtained from the Molecular Dynamics of the Protein-Ligand complex. The atoms in the protein matrix and the ligand bound to the protein are calculated to assess RMSD value. For the course of the Molecular Dynamics simulation, a number of additional factors, including Rg (Radius of Gyration), SASA (Solvent Accessible Surface Area), and hydrogen bond analysis, were also taken into account.

To calculate and analyze these parameters utilities used are gmx-rms (RMSD), gmx- rmsf (RMSF), gmx-gyrate (Rg), gmxhbond (Hydrogen bond) and gmx-sasa (SASA) (Yaraguppi et al., 2022). All the calculations are performed using the commands implemented in Gromacs (Mohammadi et al., 2016). The whole trajectory and the optimized system are utilized to generate the RMSD plot. To consider, parameters like RMSF, Rg (Radius of Gyration), SASA and H-bond, the stability index of residues in the system is used. To generate data for plotting, the whole path of 500 ns is subdivided into portions of 50 ns and is done so to make the plot easier to be analysed than a continuous stretch of 500 ns. Tools such as PyMol Tool and Visual Molecular Dynamics (VMD) are used to analyse and display data procured from the simulation. xmgrace tool is used to generate the plots and graphs obtained from simulation (Yaraguppi et al., 2022).

2.6. Molecular Mechanics Poison Surface Area analysis (MMPBSA)

The MM-PBSA approach evaluates the protein's binding free energy (ΔG binding). The g_mmpbsa an open source tool is implemented for determining interaction potentialof drug molecules throughout the stable structure of the simulation. GROMACS utility g_mmpbsa tool (https://rashmikumari.github.io/g_mmpbsa/) is used to perform calculations (Taidi et al., 2022). Using the aforementioned tool, the MM-PBSA technique is employed to evaluate different binding energy components, taking into account the entropy contribution and energy involvement of each amino acid

using the energy deposition strategy. For computing of ΔG the last 50 ns of trajectory from simulations are considered because last 50 ns are stable in the simulation and that region is calculated for MMPBSA. Through the MMPBSA calculation, additional evidence is gathered to validate the outcomes of the complex simulation. The variation between the ligand bound and ligand-free conformations of the protein is utilized to compute the unbound interaction affinity of the inhibitor with the protein. The formula presented below is employed for this purpose.

ΔG binding = G – complex – (G-protein + G – Ligand) (Yaraguppi et al., 2022).

2.7. Evaluation of anti-inflammatory activity of Urolithin a

2.7.1. In-vitro COX-2 assay

A 96-well flat bottom microplate is seeded with the breast cancer cell line MCF-7 at a density of $\sim 1 \times 10^5$ cells per well. The cells are kept at 37.2° C. and 95% humidity and 5% CO_2 over the course of the night. The cells are incubated for 24 h with Urolithin A at doses between 1 and 10 M. After giving the cells two washes in Dulbecco's phosphate-buffered saline solution, 1 mL of extraction buffer is added. The cells are recovered using a cell scraper and then, they are centrifuged at 10,000 rpm for 10 min at 4 °C. The supernatant is gathered and stored for later analysis. A human COX-2 ELISA kit was utilized and adhering to the manufacturer's guidelines, the in vitro COX-2 inhibition experiment is performed. 100 μL of collected supernatant is added to each well (control and treated sample) in duplicates followed by incubation at room temperature for 2.5 h. After being discarded, the solution is four times cleaned with 1X wash solution. The residual wash buffer is then removed by decanting or pirating following the final wash. Inverted plate is blotted with fresh paper towels. Each well is added with 100 μL of 1X biotinylated antibody before being incubated for 60 min at room temperature with light shaking. After discarding the solution, the washing process is repeated.

Each well is added with 100 μL of streptavidin solution, which is then incubated for 45 min at room temperature while being gently shaken. After discarding the solution, the washing process is repeated.Then each well is added with 100 μL of TMB (3,3′,5,5′-tetramethylbenzidine) one-step substrate reagent, which is then incubated for 30 min at room temperature under dark conditions with gentle shaking. 50 μL of stop solution is introduced to each well and immediately read at 450 nm. 10 μL of ATP-2Na solution (40 mM) is included in each well with thorough mixing and incubated at 37 °C for 30 min. The samples are retrived, and the wells are rinsed three times with washing buffer. Then, 100 μL of blocking solution is applied to individual well and incubated at 37 °C for 30 min. subsequently, the antibody solution is removed, and the wells are rinsed four times with a washing buffer. 100 μL of HRP substrate solution (TMBZ) is added in each well and incubated at 37 °C for 30 min. Lastly, 100 μL of stop solution is added to each well in the same sequence as the HRP substrate solution, and the absorbance at 450 nm is determined using a microplate reader (Nesaragi et al., 2021). The percentage (%) inhibition is calculated as follows:

$$\%\mathrm{Inhibition} = (\mathrm{Abs\ of\ sample}/\mathrm{Abs\ of\ control}) \times 100$$

The IC$_{50}$ of Urolithin A is calculated by taking the inhibition percentage of COX-2 at five different concentrations of treatment (6.25–100 μg/mL). Acetylsalicylic acid, Uridine are used as standards. Analysis is carried out in triplicates.

2.7.2. Reduction of protein denaturation

The reduction of protein denaturation using bovine serum albumin (BSA) is carried out to assess the anti-inflammatory property of Urolithin A at different concentrations following the method of

Akhter et al., (2022). Briefly, 200 μL of UrolithinA (50–500 μg/mL) prepared in dimethyl sulfoxide (DMSO) is added to 2 mL BSA (0.4% w/v prepared in PBS (phosphate buffered saline pH 7.5). The reaction solution is incubated in the thermostat water bath at 37 °C for 20 min, and then subjected to heating at 60 °C for 30 min. The solution is cooled down under laboratory conditions and absorbance is recorded at 660 nm using UV–Vis spectrophotometer. DMSO is used as negative control and assayed in a similar manner. The reduction in protein denaturation using egg albumin is also evaluated using the described procedure of Akhter et al. (2022). The assay constituted of 2 mL of Urolithin A (50–500 μg/mL), 0.2 mL of egg albumin and 2.8 mL of phosphate buffer. The reaction is incubated at 40 °C for 20 min. and heated at 70 °C for 10 min. The mixture is cooled under laboratory conditions and the absorbance is measured at 660 nm (UV Spectrophotometer).The percentage reduction in protein denaturation by Urolithin A is evaluated employing the equation reported byAkhter et al. (2022).

3. Results

3.1. Natural compounds Prediction

Owing to the consumption of pomegranate by humans and animals, the gut microbiota *Gordonibacterurolithinfaciens* sp. and *Ellagibacterisourolithinifaciens* produces Urolithins which are small metabolites. Natural gut microbial compound Urolithin A can be a very good candidate for the synthetic drug. Canonical SMILES and structure obtained for Compound ID: 5488186. The PubChem database result for Urolithin A is provided in Supplementary information. The 2D and 3D structure of Urolithin A is depicted in Table 1. The ligand of interest Urolithin A is checked for pharmacological effects from the PASS server website (https://way2-drug.com/passonline/). The PASS-SERVER results show Urolithin A to have good Anti-Inflammatory activity with Pa value of 0.572 and Pi value of 0.038. The results suggest that Urolithin A, the main metabolite of Pomegranate has emerged as a good synthetic drug candidate.

3.2. Binding site assignment and target Prediction

The COX-2 has shown three regions in its crystalline form for the selective binding of ligands. The first one corresponds to the hydrophobic pocket responsible for Arachidonic acid (AA) catalysis by TYR-385 inducing substrate oxygenation and other amino acid residues TRP-387, GLY-526, PHE-518, LEU-384 and SER-530 bound to make up this pocket. The second segment comprises the access point of the active site engaged in substrate capture, and the cavity is surrounded by the hydrophilic amino acid ARG-120, which is supported by TYR-355. The third pocket is bound by HIS-90, ARG-513, VAL-523, LEU-352, GLN-192 and SER-353. The third portion is a side chain accountable for specificity. PHE 518 is recognized for enhancing COX catalysis due to its close proximity to C-14 through C-20 of AA, as it accesses a hydrophobic region within the pocket that contributes to selectivity. This hydrophobic environment is provided by VAL-523 and the amino acids HIS-90, ARG-513, GLN-192 and SER-353.

3.3. Pharmacokinetic property analysis

The analysis for Lipinski's rule of five revealed that Urolithin A had qualified all of Ro5 parameters. The oral drug absorption included BBB which demonstrates that ligands should have CNS inactive less than 1, Caco-2 cell permeability demonstrated if the selected molecule had moderate permeability (4 ~ 70),the %HIA should be>90% for good intestinal absorption.. The results showed

that Urolithin A surpasses all the parameters to be a good drug candidate. The results of Lipinski's rule, ADMET properties and Toxicity test values for Urolithin A molecule are provided in Supplementary information.

3.4. Molecular docking

We performed a re-docking for RCX ligand associated with the crystallographic structure in the enzyme active site. The docking score was −6.26 kcal/moland is depicted in Fig. 2.

Identification of the affinity between the human COX-2 protein and selected ligand molecule (Urolithin A) and COX-2 inhibitors like acetylsalicylic acid, ibuprofen, naproxen, ketorolac and indomethacin is done using *in-silico* molecular docking approach method. The docking is executed by employing the AutoDock academic version software with MGL tools. The hCOX-2 receptor entity is prepped for the ligand–protein docking procedure through eliminating surplus water molecules, incorporating polar hydrogen atoms, combining nonpolar hydrogen atoms, and incorporating and dispersing charge. The processed receptor molecule and Ligand molecule are saved in *.pdbqt format using Autodock software. The docking simulations are validated at each stage by assessing input file names and the layout of grid maps. The generation of grid box is requisite in docking process, and has been done by centering all ligand conformations and setting up the grid box to x, y and z directions while referring the active sites in protein. The grid coordinates used during docking are provided in Table 2.

Molecular docking study is performed to get acquainted with the best interactions between Urolithin A and COX-2 binding region. The docking process is run for the 10 best poses for the protein–ligand complex. The configurations are selected as per the ligand binding energy cluster outcomes and number of hydrogen bonds. Fig. 3 showcases the visuals of binding interaction produced by PyMol software (Version 2.3).

The docking result show that Urolithin A interacts with active amino acids such as TYR 355, PHE 518, ILE 517and GLN 192 of COX-2 receptor with interaction distances of 2.8 Å, 2.3 Å, 2.5 Å and 1.9 Å respectively. The interacting amino acids of molecular docking are provided in Fig. 4. The confirmation of docking accuracy relies on assessing the interactivenessof the co-crystallized ligand, with the interactions of the test compound occurring in the identical pocket as the co-crystallized ligand. The Ligand is seen to bound with hydrophobic residues PHE518 and ILE 517, GLN192 of selective region and TYR355 at the active site. The ligand of interest shows a high docking score of −7.97 kcal/mol. The ligand-receptor interaction analysis for the ligand of interest [Urolithin-A] and with other COX-2 inhibitors with the COX-2 protein are provided in Table 3.

Redocking of COX-2 with RCX ligand in protein is seen to have a docking score of-6.27 kcal/mol. Urolithin A proves to be better COX-2 inhibitor when compared with other mentioned inhibitors in Table 3.

3.5. Molecular Dynamics and simulations

Both the solitary protein and the COX-2docked with Urolithin A and Aspirin as standard (STD) is subjected to dynamics study for the production run of 500 ns simulations. The technique of Molecular Dynamics simulations process helps in force calculation and to know the motion of amino acids atoms. Based on the several parameters such as RMSD (Complex-Ligand), RMSF, SASA, Rg and interactions with hydrogen bond the stability of the docked complex is evaluated. The RMSD parameter for ligands helps in apprehending the stability of ligands in complex with the target protein. The ligandtopology file for the ligand in complex with the protein is produced using PRODRG server (https://davapc1.bioch.dundee.
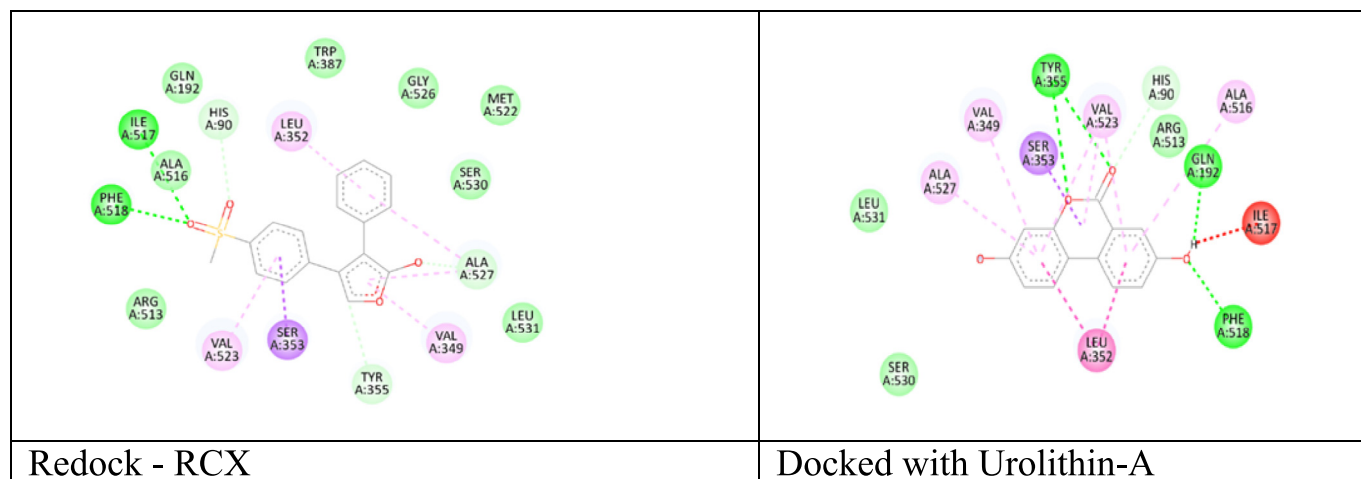
| Redock - RCX | Docked with Urolithin-A |

Fig. 2. 2D structures of Redock of COX-2 with RCX ligand and Docking with Urolithin A.

Table 2
The grid co-ordinates generated for human Cyclo-oxygenase-2 enzyme.

Protein	Dimensions	Co-ordinates	Spacing (Å)
5KIR	X- 62	X- 31.408	0.375
	Y- 72	Y- 7.993	
	Z- 58	Z- 35.311	

ac.uk/cgi-bin/prodrg/submit.html). The PDB file of the protein with APO, protein in complex with the ligands (Urolithin A, STD) is submitted to the PRODRG server and the energy-minimized topology file is generated which is used for simulation using gromacs.

The RMSD plot is generated to a known coherence of the steadiness of associated and free COX-2. The RMSD plot for APO and Protein-Ligand complexes of COX-2 is depicted in Fig. 5. During the initial 1–15 ns sharp fluctuation is observed, which is subsequently followed by obtaining a constant state of configuration for both ligand-associated and ligand disassociated complexes throughout the complete simulation. The average RMSD value is seen to be ~0.363 ± 0.54 nm for APO protein, ~0.428 ± 0.077 nm for Urolithin A and COX-2 and ~0.378 ± 0.055 nm for STD and COX-2 for the duration of 500 ns. The RMSD plot indicated the relative stability of the APO and Protein-Ligand complex in a system for the overall simulation duration of 500 ns. From the RMSD plot it is seen that Urolithin A complex has not much deviation of >1 Å ~ 3 Å difference from APO and STD complex, showing that Urolithin A is stable and equilibrated with COX-2 in entire 500 ns of simula-

tion as similar to STD with COX-2. For uniformity, the probability distribution function (PDF) of 5KIR-APO conformers wasconfined within a range of 0.31–0.49 nm, while 5KIR-URO and 5KIR-STD conformers fall within ranges of 0.39–0.53 and 0.3–0.5 nm, respectively. These findings also suggested no notable disparities in the values of PDF between the protein and protein ligand complex.

RMSF is applied to assess the consistency of amino acid residues within the protein, while also computing the residue-wise divergence of protein during entire simulation. RMSF values denote that the residue has higher flexibility and consistency only for higher RMSF values. The RMSF plot for the amino acid residues of COX-2- APO and Protein-Ligands [Urolithin A and STD] complex is shown in the Fig. 6. In the study, the fluctuations are seen for initial 1 to 100 amino acid residues. The plot for Urolithin A shows higher RMSF in many regions as similar to STD and APO, without much deviation of >1 Å ~ 3 Å difference from APO and STD complex Hence, Urolithin A molecule has a higher RMSF in the protein complex suggesting that Urolithin A is more stable and is found to be equilibrated with COX-2 throughout the simulation of 500 ns. APO and STD have also shown similar equilibration with COX-2.

The Rg values (Radius of Gyration) enables to comprehend the rigidity and compactness of the protein within the molecular dynamics system when interacting with the ligand. The average Rg value of APO and Protein in Complex with Urolithin A and STD is seen to be within the average value of ~2.400 ± 0.013 nm, ~2.378 ± 0.020 nm and ~2.388 ± 0.013 nm respectively for the duration of 500 ns of simulation as shown in the Fig. 7. It is seen
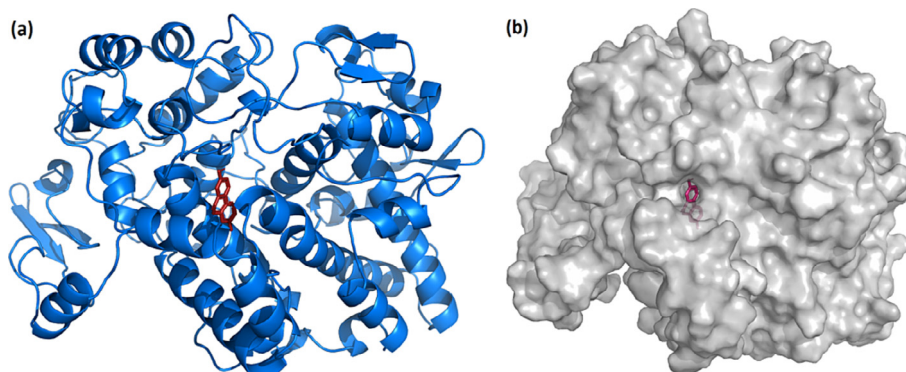

Fig. 3. Molecular Docking of Urolithin A in the binding site of Cyclooxygenase −2 (PDB ID: 5KIR) visualized using Pymol Software a) Cartoon diagram of COX-2 chain A (Blue colour) with ligand (Magenta colour); b) Surface diagram of COX-2 chain A (Grey colour) with ligand (Magenta colour).
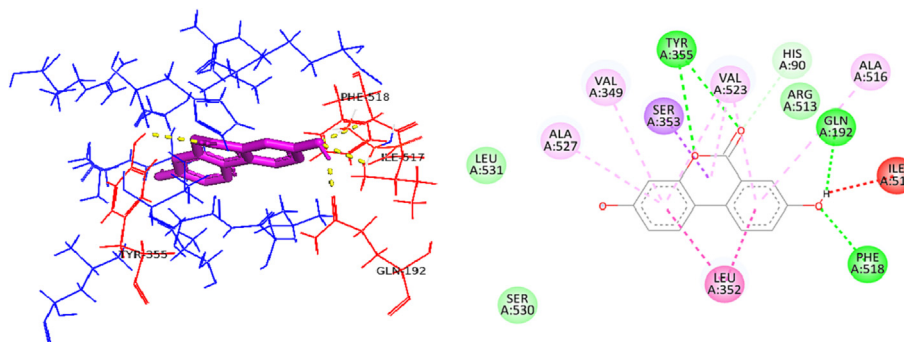
Fig. 4. Pymol Visualization of Interacting Amino acids of Molecular Docking of Urolithin A against Human Cyclooxygenase-2. Hydrogen Bonds are represented by yellow dots and 2D interaction. The Ligand is seen bounded to hydrophobic pocket residues PHE518, ILE 517, bounded by GLN192 and TYR355 at entry of active site of protein.

Table 3
Molecular Docking results of ligand Urolithin- A, Other COX-2 inhibitors with the human Cyclooxygenase-2 protein.

Ligand	Hydrogen Interacting residue	Non Polar Interactions (Hydrophobic interactions)	Binding energy (kcal/mol)
Urolithin-A	TYR-355, PHE-518, ILE-517, GLN-192	LEU359, LEU352, VAL349, SER353, THR94, HIS90, ARG513, VAL523, ALA527, ARG120, SER530, LEU531	−7.97
Acetylsalicylic acid	TYR385, SER530,GLN-192	VAL349, SER353, ALA527, ARG120	−7.54
Ibuprofen	TYR-355, PHE-518, ILE-517	LEU352, VAL349, SER353, THR94	−6.25
Naproxen	PHE-518, ILE-517, GLN-192	HIS90, ARG513, VAL523	−6.11
Ketorolac	TYR385, SER530,GLN-192	SER353, THR94, HIS90	−6.13
Indomethacin	TYR-355, PHE-518	ARG513, VAL523, ALA527,	−6.21

that Urolithin A- COX-2 complex structure displays increased compactness, resulting in enhanced stability and similar compactness is also seen with STD – Protein complex. The Rg value of Urolithin A exhibits minimal variation throughout the simulation, demonstrating its consistent compactness and stability over the entire 500 ns trajectory. PDF analysis moreover indicated a higherprobability of Rg value of 5KIR-APO compared to 5KIR-URO and 5KIR-STD.

Solvent Accessible Surface Area (SASA) is assessed to know the modulation of protein in the system. Throughout the simulation,

SASA for the complexes remained constant, equilibrated and stability is seen continuously upto 500 ns of simulation duration. The SASA for COX-2- APO, Urolithin A and Standard is seen to be around ∼ 234.66 ± 7.44 nm^2 and ∼ 236.59 ± 6.66 nm^2 and ∼ 238.39 ± 7.07 nm^2 respectively. The measurement of the change in SASA indicates the degree of aggregation of complex proteins in the system. The SASA plot for COX-2-APO and Urolithin A, STD is shown in the Fig. 8. The rise in the mean SASA value and PDF indicated that 5KIR-APO possesses a substantial solvent accessible surface area that potentially leads tohydrophobic residues exposure and subsequent protein unfolding.

Hydrogen bond analysis of COX-2 with Ligand [Urolithin A and STD] complex show that Urolithin A and STD is bound with the protein COX-2 throughout the duration. For the duration of 500 ns of dynamic simulation, a total of 3 and 4 pairs of hydrogen bonds are stable for Urolithin A and STD respectively on average of 3 positions in simulations. The presence of hydrogen throughout the 500 ns simulation duration provides evidence that Urolithin A, in complex with COX-2, maintained its integrity and equilibrium. The Hydrogen bonds formed in MD simulations are provided in the Fig. 9. From the plots of RMSD, RMSF, Rg, SASA it is seen that Urolithin A has good binding with COX-2 in its active site and stable with it for entire 500 ns of simulation duration.

3.6. MM-PBSA Prediction

MM-PBSA calculation is employed to identify the binding efficiency of COX-2 with Urolithin A and STD. The post-processing of docked complexes and rationalizing of the differences are observed after the simulation is determined by MM-PBSA. The relative binding potency is evaluated at the center of the ligand-binding site, where ligand interacts with the protein. The stability of the pro-
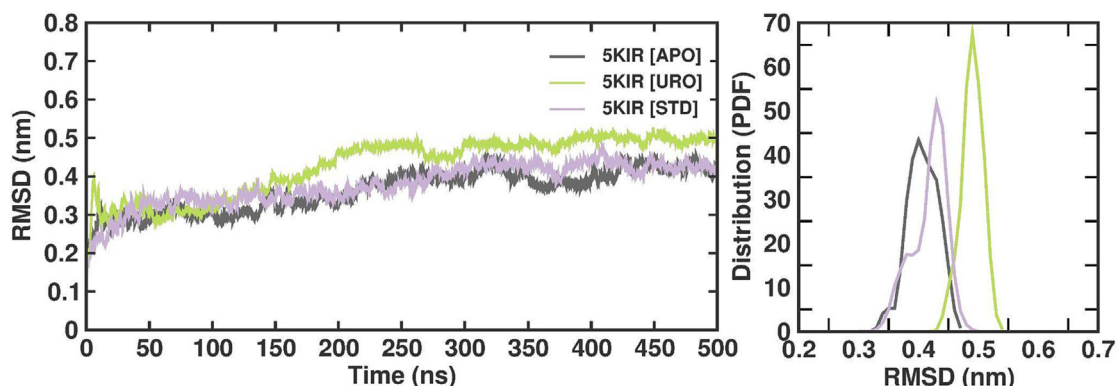

Fig. 5. RMSD plot for the APO and Protein-Ligands [Urolithin-A, STD] complex of COX-2 protein for 500 ns of simulation time.
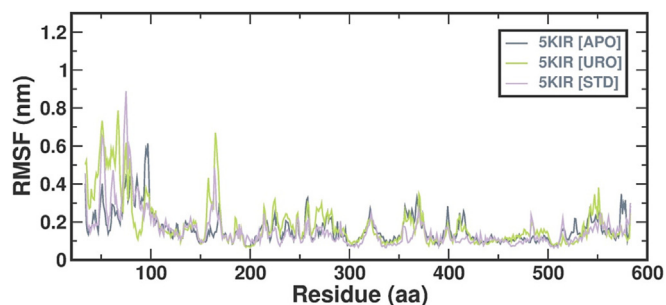
Fig. 6. RMSF plot of amino acid residues in the APO and Protein- Ligand [Urolithin A, STD] complexes.

tein–ligand complex is influenced significantly by the binding energy, and a lower energy level indicates higher stability. The data and graph illustrating the MMPBSA calculation focusing on the active site binding interactions is depicted in Fig. 10.

The findings imply that amino acid residues PHE518, GLN192, ILE517, TYR355, LEU359, VAL349, LEU352, SER353, THR94, HIS90, ARG513, VAL523, ALA527, ARG120, SER530 and LEU531 of Uro A have the greatest contribution to the total binding energy of – 22.0368 kJ/mol and STD had −20.4959 kJ/mol with COX-2. All the active site residues took part in H-bond formation and are calculated for MMPBSA pocket analysis. The molecules were present in same place throughout the simulation. The observed data indicated that the ligand molecule remain attachedto the target protein during the entire simulation, leading to the inhibition of human COX-2.

In this current study anti-inflammatory activity of Urolithin A on COX-2 is carried out by an *In-silico* approach. COX-2 integral role in the inflammation pathway involves the conversion of arachidonic acid into Prostaglandins G2 (PGG2). PGG2 increases inflammation, pain and fever.The binding energy of Urolithin A in complex with COX-2 was −7.97 kcal/mol with active residues of COX-2 binding and active sites.

3.7. Assessment of anti-inflammatory property of Urolithin A

Inflammation is a result of cellular reactions that are mediated by inflammatory agents. COX enzymes have a substantial role in biosynthesis of prostaglandins and hence are recommended targets during drug evaluation and development. COX enzyme inhibition presents a viable strategy to mitigate inflammation in the body. Anti-inflammatory agents are recognized for their specific inhibition of COX-1 and COX-2. The inhibition of COX enzymes is a possible mechanism to reduce inflammation in the body. Anti-

inflammatory drugs are known to inhibit COX-1 and COX-2 specifically. To study the anti-inflammatory effect of Urolithin A, an *In-vitro* COX-2 assay using breast cancer cell line MCF-7 is carried out. Urolithin A shows a strong, dosage-dependent inhibition of COX-2 that is evaluated in the range of 6.25–100 µg/mL as shown in Fig. 11. Inhibition percentage of COX-2 by Urolithin A is observed to be 38.5% and 79.29% at 6.25 µg/mL and 100 µg/mL concentrations respectively. The IC$_{50}$ value of Urolithin A is found to be 44.04 µg/mL in comparison to the standard Acetylsalicylic acid which showed 20.84 µg/mLand Uridine which showed 29.25 µg/ml. The results indicate that Urolithin A acts as effective suppressor of COX-2 and is comparable to standard anti-inflammatory drugs.

The anti-inflammatory potential of Urolithin A is assessed by measuring percentage reduction in protein denaturation with BSA and egg albumin in the concentration range of 50–500 µg/m L. An increased trend of percentage reduction of protein denaturation is proved with both the proteins in concentration dependent means as illustrated in Fig. 12. The protein denaturation percentage reduction for BSA ranged from 7.3 ± 0.05 to 37.6 ± 0.1 % and for egg albumin ranged from 10.8 ± 0.06 to 43.2 ± 0.07 %. The highest inhibition of protein denaturation is achieved at 500 µg/mL of Urolithin A concentration. However, further inhibition of protein denaturation may be possible by a further increase in Urolithin A concentration. Comparatively inhibitory effect on protein denaturation is better in egg albumin.

4. Discussion

Urolithins show to have benefits associated with the diet (Dellafiora et al., 2020; Jing et al., 2019). The research on Urolithin A has shown to be effective in anti-inflammatory activity, blocking of S-glycoprotein of SARS-CoV-2, interacting with Covid-19 proteases and neuroprotective activities (González-Sarrías et al., 2010; Suručić et al., 2021; Ahmad, 2020; Ahsan et al., 2019).Urolithins exhibitspotent antioxidant property compared with that of ascorbic acid. In an*in vivo* study by ORAC method of large number of polyphenols and their metabolites, Urolithin A showed powerful anti-oxidant activity (Espín et al., 2013; Djedjibegovic et al., 2020). Urolithin's ability to behave as enterophytoestrogens were studied, the structure activity showed that Urolithins A and B had particular molecular features that made it possible for these molecules to connect to α and β- estrogenic receptors (Espín et al., 2013). By blocking the MMP-9 enzyme, urolithins produce antimalarial action. In hemozoin and TNF- stimulated monocytic cells, urolithins A and B reduced MMP-9 release and its mRNA expression at lower doses. These findings suggested that urolithins may contribute to the antimalarial effects of pomegrante rind. The
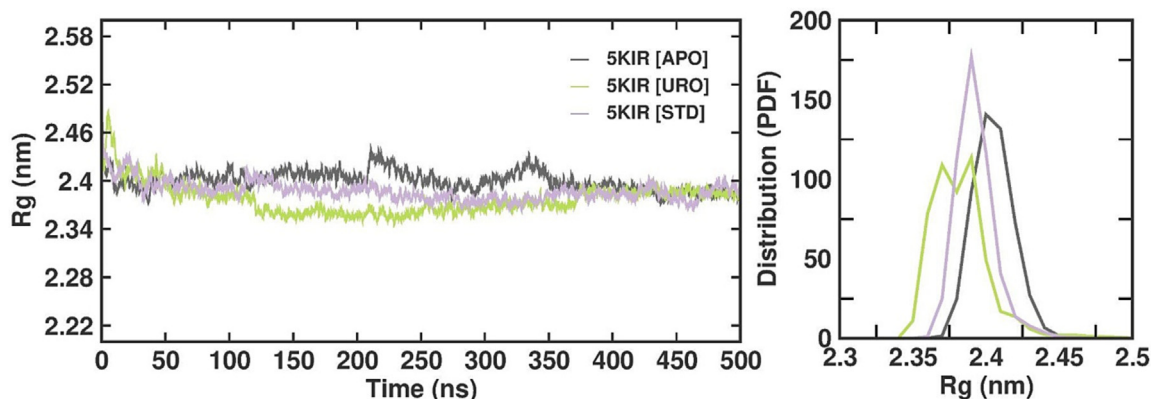

Fig. 7. Radius of gyration plot showing the compactness of APO, Urolithin A, and STD complex throughout the simulation duration.
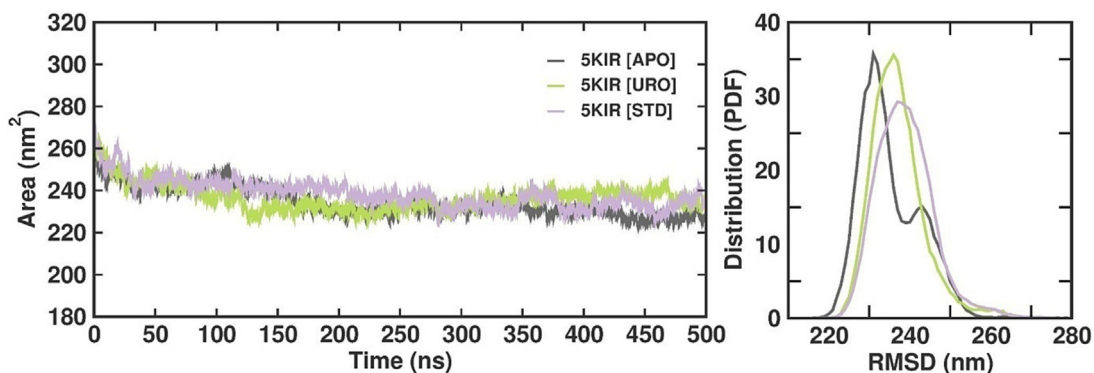
Fig. 8. Plot of SASA value vs time for Cyclooxygenase 2- APO, Urolithin A, and STD complex.
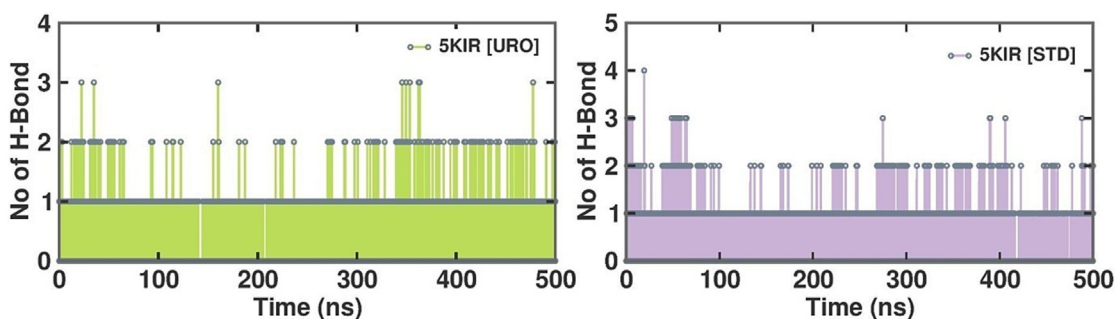

Fig. 9. Number of Hydrogen bonds formed for the trajectory of MD simulation for Cyclooxygenase-2 enzyme with Urolithin A and STD.
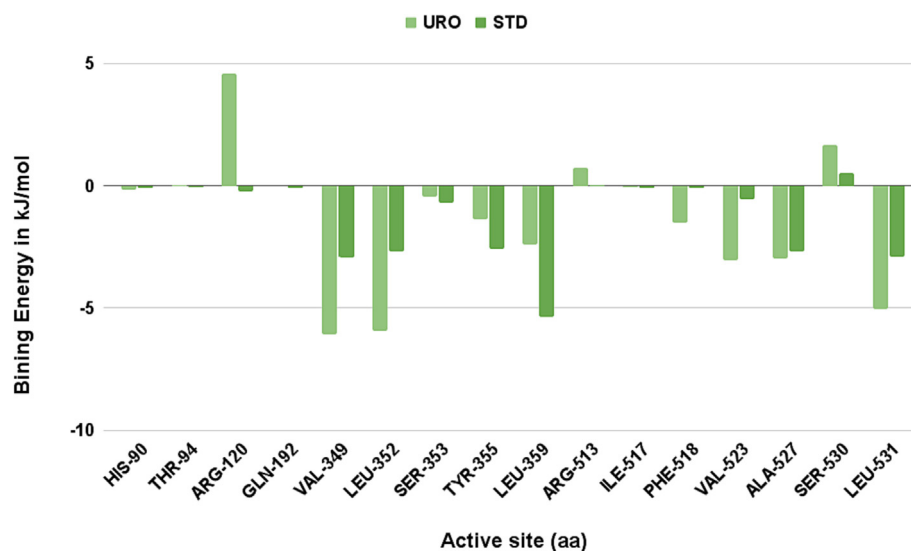

Fig. 10. Active Site-level interaction energy (Binding energy) from MM-PBSA in the simulation.

ubiquitous protein kinase CK2 is inhibited by urolithins, which can disrupt a range of cellular processes and result to conditions including cancer and inflammation. The metabolites urolithin A and B, which are generated from microbiota, may have antipathogenic actions in the colon against *Y. enterocolitica* through Quorum sensing inhibition and the microbial equilibrium is maintained in colon gut (Espín et al., 2013).

Over the recent years, there has been a notable surge in in-vivo investigations employing animal models to showcase biological functionalities subsequent to the administration of Urolithins. These studies have encompassed oral as well as intraperitoneal delivery methods, effectively substantiating their engagement in the advantageous outcomes ascribed to the consumption of ellag-itannin – rich dietary sources (García-Villalba et al., 2022). Research studies indicate that the administration of Urolithin A exhibits the ability to safeguard against or mitigate injury caused by inflammation in various inflammation models. These models encompass scenarios like ischemia/reperfusion injury and osteoarthritis. This protective effect is correlated with the reduction of systemic pro-inflammatory cytokines and the attenuation of signalling pathways that become heightened under inflammatory conditions (García-Villalba et al., 2022).
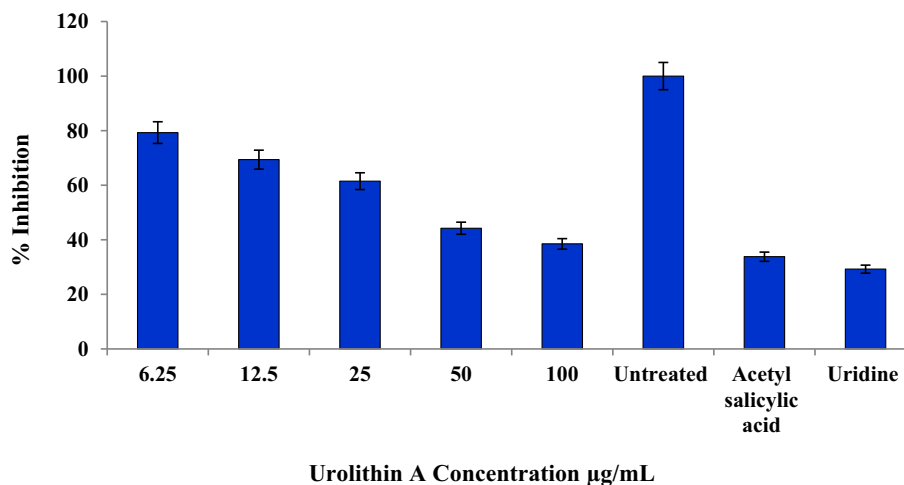
Fig. 11. Anti- inflammatory activity of Urolithin A by *In-vitro* COX-2 assay.
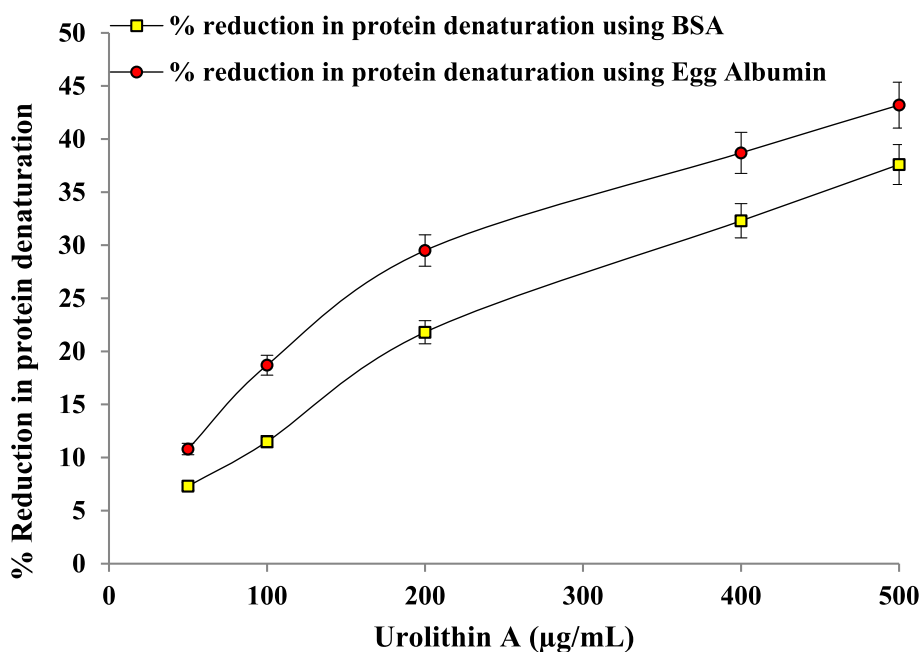

Fig. 12. Anti-inflammatory activity of Urolithin A by Reduction of protein denaturation using BSA and egg albumin.

In recent times, a multitude of investigations have commenced elucidating the potential role of Urolithins in contributing partially to the favourable outcomes linked to the consumption of ellagitannin – rich foods against neurodegerative disorders such as Alzheimer's or Parkinson's disease (García-Villalba et al., 2022).The emergence of *Gordonibacter urolithinfaciens* species nova has been attributing its role in conversion of elagic acid into urolithin M5 and Urolithin C. This microorganism belongs to *Coriobacteriaceae* family, a lineage closely associated with advantageous effects in relation to obesity (Kang et al., 2016). Urolithin A exhibits a rejuvenating impact on aged human skin fibroblasts, leading to an augmentation in the production of type 1 collagen while concurrently impeding the expression of matrix metalloprotease-1 (Zhang et al., 2022). In a recent study conducted exploration of urolithins potentiality as viable remedies for diabetes, Urolithin C emerged as the most potent molecule (Bayle et al., 2016).

According to a review of the literature, COX-2, a crucial enzyme involved in the production of prostaglandin G2 (PGG2) from arachidonic acid during inflammation, can be inhibited. The tried ligand compound Urolithin A proves to be a good inhibitor by exhibiting strong binding affinity with the desired protein COX-2 (Taidi et al., 2022). In the present researchUrolithin A showed good binding activity with docking score of −7.97 kcal/mol whereas other COX-2 inhibitors like Mefenamic acid, MAM (an ester of mefenamic acid and menthol) exhibited docking score of −7.67 kcal/mol and −7.27 kcal/mol respectively (Shah et al., 2019), Kuwanon A had a docking score of −7.044 kcal/mol with great affinity towards ARG120 and TYR-355 at the opening of the active site of COX (Baek et al., 2021), Eugenol and Aspirin when docked with COX-2 showed a docking score of −6.69 kcal/mol and −7.45 kcal/mol respectively (das Chagas Andrade and Mendes, 2020).

COX-2 inhibitors Rofecoxib, compounds Z814 and Z627 have shown binding affinity value of −48.15 kcal/mol, −45.5115 kcal/mol and −42.7615 kcal/mol respectively (Araújo et al., 2020). 1-(4-(6-methoxy-2-naphthoyl)-1-phenyl-1H-pyrazol-3-yl) ethan-1-

one a synthesized compound that had COX-2 inhibiting activity showed binding energy of −34.8 kJ/mol (El Sayed et al., 2018).

The binding energy result in current research seems to be favorable when compared with several other studies on COX-2 by ligands like Eugenol (Cerdá et al., 2005), and Eutyploids (Taidi et al., 2022). The commercial NSAIDs of COX-2 shows that blocking of binding or active sites is shown to inhibit COX-2 (Orlando and Malkowski, 2016). The inhibition of COX-2 also inhibits the adverse effects of prostaglandins in eroding inflammation. Urolithin A shows binding with COX-2 at residues PHE518, TYR355, ILE517 and GLN192. PHE518 is one of the residues of the hydrophobic pocket that is laible for the catalysis of Arachidonic acid, TYR355 is the residue of entry of the active site and GLN192 is the residue of the lateral chain responsible for selectivity (Taidi et al., 2022). So blocking of these main residues around the active site is regarded as a good competitor for inhibiting the human COX-2 that plays a major role in inflammation. Amino acid residues PHE518, GLN192, ILE517, TYR355, LEU359, VAL349, LEU352, SER353, THR94, HIS90, ARG513, and ARG120 knownPhytocompounds of the kuwanon class of compounds from *Morusalba*L.are seen to have effective blockage of the active site of COX-2, and the same site is seen to be blocked in the current study (Baek et al., 2021).

The compound Urolithin A considered in this study is well known for its stability based on Fukui function and also for its consistent activity shown both by In-silico and experimental studies hence making them a highly drug-like compound (Hussein and Azeez, 2023).Urolithin A in terms of chemical reactivity and stability properties calculated using Frontier Molecular Orbitals (FMO) makes it an excellent drug candidate for therapeutic applications (Hussein and Azeez, 2023). Urolithin A is present in various plant sources which are widely considered as healing food in traditional medicine and are used for curing ulcers and inflammatory disorders (Ahmad, 2020).

Reports suggest that several side effects prevail through the inhibition of COX-1 such as, gastrointestinal disease, risk associated to cardiovascular disease, bleeding etc. Hence the research on synthesis of drugs that specifically target COX-2 is gaining focus (Baek et al., 2021). Urolithin A is considered as a selective COX-2 inhibitor. Similar to our results, previous study by Nesaragi et al., (2021) have reported that the synthesized compounds possessed more selectivity towards COX-2 inhibition in comparison to COX-1 inhibition and correlated with the docking studies. The study also revealed that drugs with halo substituents may have inhibitory effects on COX-2 and have better selectivity toward COX-2 than COX-1.

Previous studies are evident regarding the inhibitory effects of pomegranate fruit extract constituents or metabolites on COX enzymes. These compounds are found to be more bioavailable through systemic circulation and are potent, significant and less toxic inhibitors of COX-2 (Shukla et al., 2008). The COX inhibitory potential of urolithins are evaluated by Noshadi et al., (2020) which indicate that the active compounds had 1,3,8-trisubstitution that displayed prominent inhibitory features in comparison to the known COX inhibitors. Several mechanisms are reported for the inhibitory effects such as, treatment with Urolithin A leading to suppression of expression of COX-2, PGE2, NO, TNF-α, IL-6 and inducible nitric oxide synthase (iNOS). Urolithin A participates in signalling pathways and hinders NF-κB and PI3K/Akt, providing protection against IL-1β-induced degradation. Urolithin A also engages in suppressing cytokines in macrophages by blocking NF-κB translocation, thereby halting the transcription of genes involved in pro-inflammatory cytokine production (Noshadi et al., 2020). The In-vitro analysis is consistent with the outcomes of In-silico studies.

Bobowska et al., (2021) assessed the anti-inflammatory response of urolithin A, iso-urolithin A and urolithin B, along with their glucuronides towards altering the immune response in THP-1 derived macrophages, RAW 264.7 macrophages, PBMCs – derived macrophages and primary neutrophils. The most effective metabolite for inhibiting the LPS – induced inflammatory response (TNF-α attenuation, IL-10 induction) was determined to be urolithin A. Its mechanism of action is hypothesized to involve the strong induction of ERK 1/2 phosphorylation. In terms of pro-inflammatory TNF – α inhibition and anti-inflammatory IL-10 and TGF-1 induction, none of the evaluated glucuronide conjugates were effective. In a study an assumption was made that Urolithins might influence the synthesis of inflammatory eicosanoids derived from leukocytes, within the context of the 5-lipoxygenase (5-LOX), Cyclooxygenase – 2 (COX-2), and 5-LOX/COX-2 pathways. This modulation is thought to have relevance in both the initiation and progression of inflammatory bowel diseases (IBDs), encompassing compounds such as 5-hydroxyeicosatetraenoic acids (5-HETEs), leukotriene-B4 (LTB4), prostaglandin E2 (PGE2) and hemiketals (HKE2 and HKD2). It was found that Uro-A, isoUro-A and Uro-C exhibited the ability to disrupt the 5-LOX/COX-2 cascade, leading to a decrease in the production of the hemiketal eicosanoids HKE2 and HKD2, following a concentration dependent manner (Giménez-Bastida et al., 2020).

Karim et al., (2023)noted hepatoprotective effects that may have been caused by Uro A anti-inflammatory action, which resulted in lower production of two important inflammatory cytokines TNF-α and IL-6.Lee et al., (2019) reported Urolithin B inhibited the production of nitric oxide and pro-inflammatory cytokines, leading to a simultaneous enhancement in the expression of the anti-inflammatory cytokine IL-10 within lipopolysaccharide stimulated BV2 microgial cells. By decreasing intracellular ROS production and NADPH oxidase subunit expression while increasing the expression of the antioxidant hemeoxygenase-1, urolithin B also demonstrated an anti-oxidant effect.

The current study also fortifies the exploration of existing literature, focusing on the molecular dockings of closely related anti-inflammatory compounds. By delving into the molecular interactions and binding affinities of these analogous molecules, it is used to bolster the rationale behind ligand selection and highlight the potential significance of Urolithin A within the context of anti-inflammatory mechanisms. This strategic incorporation of prior molecular docking analyses offers a robust foundation for current research direction and lends credibility to the pathway pursued. Hikmaranti et al., (2020) assessed anti diabetic and anti-inflammatory potential of Gallic acid, Ellagic acid, Urolithin A and Urolithin B with NF-κB protein by In-silico approach. All the four compounds could bind to active site of NF-κB indicating their potentiality in inhibiting protein activity. The compound ellagic acid exhibited the most favourable binding energy, indicating that it is most stable among the compounds assessed. This characteristic also signified its heightened capacity for activating the NF-κB pathway's inhibition. It was inferred that ellagic acid demonstrates superior efficacy in regulating the transition of NF-κB from the cytoplasm to the nucleus by virtue of its interactions with ligands binding to amino acid residues (Tyr36, Lys37, Cys38 and Lys122) within the active site of the NF-κB complex. This mechanism served to hinder the translocation of NF-κB from the cytoplasm to the nucleus, contributing to its role in preventing inflammation.

An anti-inflammatory study of phytochemicals from selected plants *Carica papaya*, *Punica granatum*, *Citrus limon*, *Curcuma longa*and *Dalbergia sisso* on cyclooxygenase 2 was tested using molecular docking. *Punica granatum*'s 1,2,6- Trigalloylglucose showed the best molecular docking scores against COX-2, that supported its active role in the anti-inflammatory effects it provides in pome-

granate juice (Rana et al., 2019). The principal constituents (including ellagic acid, gallic acid, quercetin, punicalgin, punicic acid, ascorbic acid, kaemferol and naringin) present within the pomegranate rind portion were subjected to molecular docking analysis against receptors associated with anti-inflammatory and anti-apoptotic processes, such as IL-1, IL-6, IL-10, Bcl-2, Bax and caspase-3. Punicalgin emerged to exhibit the least binding energy values for IL-1 (−11.6), IL-6 (−10.6), IL-10 (−11.7), Bcl-2 (−10.8), Bax (−10.4) and apoptotic marker caspase-3(-10.1). These results emphasize the remarkable capacity of punicalgin in relation to its exceptional potential for both anti-inflammatory and anti-apoptotic efficiency (Karwasra et al., 2016).

Refaey et al., (2022) reported that by enhancing COX-2 and reducing TNF- α levels, the major components camphor and *trans*-thujone of essential oil derived from various parts of *C.anthemoides* (CAEO) suppress the inflammatory response in LPS stimulated RAW 264.7 cells. The presence of bornyl acetate, *cis*-para-Menth-2-ene-1-ol and *cis*-β-Farnesene, which could be used as lead compounds for the discovery of a selective anti-inflammatory drug, attributed to this activity by the molecular docking results. Being a natural anti-inflammatory and available in variety of dosage forms, CAEO can be used in pharmaceutical goods. An anti-inflammatory activity of guanine dimers isolated from the *Xylopia vielana* was evaluated by Molecular docking, ADMET studies and Dynamic simulations aganist COX-2 protein. The study showed all isolated compounds possessed inhibitory activity against COX-2. Further analysis of the compound xylopidimer C involved MD simulations, and its molecular interactions with the COX-2 revealed clear interactions with the active groups of the enzyme through hydrogen bonding as well as hydrophobic contacts. Notably, xylopidimer C displayed the highest binding affinity, with −10.57Kcal/mol energy with 17.92 nanomolar of predicted inhibition constant surpassing the performance of both Ibuprofen and Felbinac (Hassan et al., 2022).

Alam et al., (2021) studied the antioxidative and anti-inflammatory properties of essential oil from *Guatemala cardamom* (GCEO). They conducted assays using 2,2-diphenyl-1-picrylhydrazyl-hydrate, ferric-chloride, bovine serum albumin and proteinase inhibitors, highlighting α-terpinyl acetate and 1,8-cineole as principal constituents demonstrating noteworthy effects. Through molecular docking, the substantial binding affinity of both components to human peroxiredoxin-5, tryrosine kinases, and human 5-LOX receptors was uncovered. Computational activity prediction analysis further validated the antioxidant and anti-inflammatory potentials.

A previous safety assessment study of Urolithin A by Heilman et al., (2017), reported in their study that Urolithin A is not genotoxic. Urolithin A dosage study are performed for 28 days (0%, 0.175%, 1.75% and 5%) and 90 days (0%, 1.25%, 2.5% and 5%) and it is noted for no changes in clinical parameters, blood chemistry, or any indication of target organs or specific toxic mechanisms caused by Urolithin A, as demonstrated by the evidence. The IC_{50} value (44.04 μg/ml) of Urolithin A has not exceeded the highest concentration of dosage that is reported in study byHeilman et al., (2017). Jeengar et al., (2017) carried out a study on treatment of Uridine on Dextran Sulfate Sodium (DSS) – Induced colitis in mice and observed a significant reduction of protein expression of TNF-α, COX-2, IL-6, P-NFkB and colon tissue myeloperoxidase activity when treated with medium and high dose groups.

It has been found that, the thermal protein denaturation can induce the production of auto-antigenic proteins that participate in the autoimmune reaction leading to a diseased state of the body and also trigger the variations in disulphide, hydrogen and electrostatic hydrophobic bonding patterns (Akhter et al., 2022). In the present investigation, Urolithin A shows a pronounced reduction in the thermally induced protein denaturation process indicating

a subsequent inhibition in the synthesis of auto-antigenic proteins involved in the inflammation. Similar to our study, noscapine hydrochloride also shows a notable reduction in the heat-induced protein denaturation of egg albumin and BSA. Noscapine hydrochloride administration has been shown to drastically lower COX-2 expression, decrease NF-kB expression, and block the mRNA expression of pro-inflammatory biomarkers (Akhter et al., 2022).

Several plant extracts have also been reported to produce an inhibitory effect on BSA protein denaturation thereby identifying potential lead in anti-inflammatory plant-based compounds. The protein denaturation is regarded as a process that triggers the loss of configuration and functionality thereby recommending the suitability of the *In*-vitro assay for analysis of anti-inflammatory properties (Bailey-Shaw et al., 2017).

In another study, tryptophan fluorescence spectroscopy is utilized as a vital approach to examine the protein denaturation inhibition by herbal derivatives. BSA is commonly used to evaluate protein denaturation as it is a globular protein harbouring aromatic amino acids (tryptophan, tyrosine and phenylalanine) that are well known to be fluorescent. During the denaturation progression, the increased fluorescence intensity indicates the extent of protein unfolding (Sharma et al., 2021).

5. Conclusion

This study involved Urolithin A metabolite of ellagitanninthat inhibited human COX −2 by*In-silico* approach. COX-2 is the main protein that paves way for the progression of inflammation by converting Arachidonic acid into Prostaglandins G2 inhibiting COX-2 directly impacting inflammation. Urolithin A demonstrates encouraging outcomes, displaying potent inhibition of COX-2 enzyme while exhibiting favourable pharmacokinetic properties, absence of toxicity, and strong binding affinity to the active site residues such as TYR355, PHE518, ILE517 and GLN192 of the protein with a binding energy of −7.97 kcal/mol. Molecular Dynamics study also shows stable binding between protein and ligand for a simulation duration of 500 ns. The total binding energy of −22.0368 kJ/mol is observed through MMPBSA for hydrophilic and hydrophobic interactions. To verify the validity of the in-silico molecular docking simulation approach, the acquired in-silico findings are compared with previously published experimental pharmacological data. Also, the anti-inflammatory effect of Urolithin A is validated through *In-vitro* COX-2 assay and reduction of protein denaturation and is significantly evident in dose dependent manner. It is found that molecular docking, simulation studies for 500 ns duration results for Urolithin A and COX-2 complex was stable and supported by wet lab results with IC_{50} value of 44.04 μg/ml by *In-vitro* COX-2 assay and 37.6 ± 0.1 % and 43.2 ± 0.07 % reduction of protein denaturation for BSA and egg albumin respectively at 500 μg/ml. The outcome of the current study conveys the innovativeness of computational and *In-vitro* studies of Anti-inflammatory activity of Urolithin A on COX-2 thus providing knowledge to scientific field.

CRediT authorship contribution statement

Archana G. Revankar: Data curation, Investigation, Methodology, Validation, Writing – original draft. **Zabin K. Bagewadi:** Data curation, Investigation, Methodology, Supervision, Writing – review & editing. **Ibrahim A. Shaikh:** Resources. **Basheerahmed Abdulaziz Mannasaheb:** Validation. **Mohammed M. Ghoneim:** Validation. **Aejaz Abdullatif Khan:** Validation. **Sayed Mohammed Basheeruddin Asdaq:** Validation.

Declaration of Competing Interest

The authors declare that they have no known competing financial interests or personal relationships that could have appeared to influence the work reported in this paper.

Appendix A. Supplementary material

Supplementary data to this article can be found online at https://doi.org/10.1016/j.sjbs.2023.103804.

References

Ahmad, V., 2020. A molecular docking study against COVID-19 protease with a pomegranate phyto-constituents "Urolithin" and other repurposing drugs: from a supplement to ailment. J. Pharm. Res. Int., 51–62 https://doi.org/10.9734/jpri/2020/v32i1130545.

Ahsan, A., Zheng, Y., Wu, X., Tang, W., Liu, M., Ma, S., Jiang, L., Hu, W., Zhang, X., Chen, Z., 2019. Urolithin A-activated autophagy but not mitophagy protects against ischemic neuronal injury by inhibiting ER stress in vitro and in vivo. CNS Neurosci. Ther. 25, 976–986. https://doi.org/10.1111/cns.13136.

Akhter, S., Irfan, H.M., Alamgeer, U.A., Jahan, S., Roman, M., Latif, M.B., Mustafa, Z., Almutairi, F.M., Althobaiti, Y.S., 2022. Noscapine hydrochloride (benzyl-isoquinoline alkaloid) effectively prevents protein denaturation through reduction of IL-6, NF-kB, COX-2, Prostaglandin-E2 in rheumatic rats. Saudi Pharm. J. 30, 1791–1801. https://doi.org/10.1016/j.jsps.2022.10.008.

Alam, A., Jawaid, T., Alam, P., 2021. In vitro antioxidant and anti-inflammatory activities of green cardamom essential oil and in silico molecular docking of its major bioactives. J. Taibah Univ. Sci. 15, 757–768. https://doi.org/10.1080/16583655.2021.2002550.

Araújo, P.H.F., Ramos, R.S., da Cruz, J.N., Silva, S.G., Ferreira, E.F.B., de Lima, L.R., Macêdo, W.J.C., Espejo-Román, J.M., Campos, J.M., Santos, C.B.R., 2020. Identification of potential COX-2 inhibitors for the treatment of inflammatory diseases using molecular modeling approaches. Molecules 25, 4183. https://doi.org/10.3390/molecules25184183.

Baek, S.-H., Hwang, S., Park, T., Kwon, Y.-J., Cho, M., Park, D., 2021. Evaluation of selective COX-2 inhibition and in silico study of kuwanon derivatives isolated from Morus alba. Int. J. Mol. Sci. 22, 3659. https://doi.org/10.3390/ijms22073659.

Bailey-Shaw, Y.A., Lawrence, A.D., Williams, C.E.G., Rodney, S., Smith, A.M., 2017. In-Vitro evaluation of the anti-inflammatory potential of selected jamaican plant extracts using the bovine serum albumin protein denaturation assay. Int. J. Pharm. Sci. Rev. Res., 145–153

Bayle, M., Roques, C., Marion, B., Audran, M., Oiry, C., Bressolle-Gomeni, F.M.M., Cros, G., 2016. Development and validation of a liquid chromatography-electrospray ionization-tandem mass spectrometry method for the determination of urolithin C in rat plasma and its application to a pharmacokinetic study. J. Pharm. Biomed. Anal. 131, 33–39. https://doi.org/10.1016/j.jpba.2016.07.046.

Blanco, F.J., Guitian, R., Moreno, J., de Toro, F.J., Galdo, F., 1999. Effect of antiinflammatory drugs on COX-1 and COX-2 activity in human articular chondrocytes. J. Rheumatol. 26, 1366–1373.

Bobowska, A., Granica, S., Filipek, A., Melzig, M.F., Moeslinger, T., Zentek, J., Kruk, A., Piwowarski, J.P., 2021. Comparative studies of urolithins and their phase II metabolites on macrophage and neutrophil functions. Eur. J. Nutr. 60, 1957–1972. https://doi.org/10.1007/s00394-020-02386-y.

Brune, K., Patrignani, P., 2015. New insights into the use of currently available non-steroidal anti-inflammatory drugs. J. Pain Res. 105. https://doi.org/10.2147/JPR.S75160.

Cerdá, B., Periago, P., Espín, J.C., Tomás-Barberán, F.A., 2005. Identification of Urolithin A as a metabolite produced by human colon microflora from ellagic acid and related compounds. J. Agric. Food Chem. 53, 5571–5576. https://doi.org/10.1021/jf050384i.

Chan, C.C., Boyce, S., Brideau, C., Charleson, S., Cromlish, W., Ethier, D., Evans, J., Ford-Hutchinson, A.W., Forrest, M.J., Gauthier, J.Y., Gordon, R., Gresser, M., Guay, J., Kargman, S., Kennedy, B., Leblanc, Y., Leger, S., Mancini, J., O'Neill, G.P., Ouellet, M., Patrick, D., Percival, M.D., Perrier, H., Prasit, P., Rodger, I., 1999.

Rofecoxib [Vioxx, MK-0966; 4-(4'-methylsulfonylphenyl)-3-phenyl-2-(5H)-furanone]: a potent and orally active cyclooxygenase-2 inhibitor. Pharmacological and biochemical profiles. J. Pharmacol. Exp. Ther. 290, 551–560.

das Chagas Pereira de Andrade, F., Mendes, A.N., 2020. Computational analysis of eugenol inhibitory activity in lipoxygenase and cyclooxygenase pathways. Sci. Rep. 10, 16204. https://doi.org/10.1038/s41598-020-73203-z.

Dellafiora, L., Milioli, M., Falco, A., Interlandi, M., Mohamed, A., Frotscher, M., Riccardi, B., Puccini, P., Rio, D.D., Galaverna, G., Dall'Asta, C., 2020. A hybrid in silico/in vitro target fishing study to mine novel targets of Urolithin A and B: a step towards a better comprehension of their estrogenicity. Mol. Nutr. Food Res. 64, 2000289. https://doi.org/10.1002/mnfr.202000289.

Djedjibegovic, J., Marjanovic, A., Panieri, E., Saso, L., 2020. Ellagic acid-derived urolithins as modulators of oxidative stress. Oxid. Med. Cell. Longev. 2020, 1–15. https://doi.org/10.1155/2020/5194508.

El Sayed, M.T., El-Sharief, M.A.M.S., Zarie, E.S., Morsy, N.M., Elsheakh, A.R., Nayel, M., Voronkov, A., Berishvili, V., Sabry, N.M., Hassan, G.S., Abdel-Aziz, H.A., 2018. Design, synthesis, anti-inflammatory antitumor activities, molecular modeling and molecular dynamics simulations of potential naprosyn® analogs as COX-1 and/or COX-2 inhibitors. Bioorg. Chem. 76, 188–201. https://doi.org/10.1016/j.bioorg.2017.11.002.

Elhenawy, A.A., Al-Harbi, L.M., El-Gazzar, M.A., Khowdiary, M.M., Moustfa, A., 2019. Synthesis, molecular properties and comparative docking and QSAR of new 2-(7-hydroxy-2-oxo-2H-chromen-4-yl)acetic acid derivatives as possible anticancer agents. Spectrochim Acta Part A Mol. Biomol. Spectrosc. 218, 248–262. https://doi.org/10.1016/j.saa.2019.02.074.

Espín, J.C., Larrosa, M., García-Conesa, M.T., Tomás-Barberán, F., 2013. Biological significance of urolithins, the gut microbial ellagic acid-derived metabolites: the evidence so far. Evidence-Based Complement. Altern. Med. 2013, 1–15. https://doi.org/10.1155/2013/270418.

García-Villalba, R., Giménez-Bastida, J.A., Cortés-Martín, A., Ávila-Gálvez, M.Á., Tomás-Barberán, F.A., Selma, M.V., Espín, J.C., González-Sarrías, A., 2022. Urolithins: a comprehensive update on their metabolism, bioactivity, and associated gut microbiota. Mol. Nutr. Food Res. 66, 2101019. https://doi.org/10.1002/mnfr.202101019.

Gaya, P., Peirotén, Á., Medina, M., Álvarez, I., Landete, J.M., 2018. Bifidobacterium pseudocatenulatum INIA P815: the first bacterium able to produce urolithins A and B from ellagic acid. J. Funct. Foods 45, 95–99. https://doi.org/10.1016/j.jff.2018.03.040.

Giménez-Bastida, J.A., González-Sarrías, A., Espín, J.C., Schneider, C., 2020. Inhibition of 5-Lipoxygenase-Derived Leukotrienes and Hemiketals as a Novel Anti-Inflammatory Mechanism of Urolithins. Mol. Nutr. Food Res. 64, 2000129. https://doi.org/10.1002/mnfr.202000129.

González-Sarrías, A., Larrosa, M., Tomás-Barberán, F.A., Dolara, P., Espín, J.C., 2010. NF-κB-dependent anti-inflammatory activity of urolithins, gut microbiota ellagic acid-derived metabolites, in human colonic fibroblasts. Br. J. Nutr. 104, 503–512. https://doi.org/10.1017/S0007114510000826.

Grosser, T., Theken, K.N., FitzGerald, G.A., 2017. Cyclooxygenase inhibition: pain, inflammation, and the cardiovascular system. Clin. Pharmacol. Ther. 102, 611–622. https://doi.org/10.1002/cpt.794.

Hasheminezhad, S.H., Boozari, M., Iranshahi, M., Yazarlu, O., Sahebkar, A., Hasanpour, M., Iranshahy, M., 2022. A mechanistic insight into the biological activities of urolithins as gut microbial metabolites of ellagitannins. Phyther. Res. 36, 112–146. https://doi.org/10.1002/ptr.7290.

Heilman, J., Andreux, P., Tran, N., Rinsch, C., Blanco-Bose, W., 2017. Safety assessment of Urolithin A, a metabolite produced by the human gut microbiota upon dietary intake of plant derived ellagitannins and ellagic acid. Food Chem. Toxicol. 108, 289–297. https://doi.org/10.1016/j.fct.2017.07.050.

Hermanson, D.J., Gamble-George, J.C., Marnett, L.J., Patel, S., 2014. Substrate-selective COX-2 inhibition as a novel strategy for therapeutic endocannabinoid augmentation. Trends Pharmacol. Sci. 35, 358–367. https://doi.org/10.1016/j.tips.2014.04.006.

Hikmaranti, M., Astiyani, A.M., Hasanah, K.M., Maghfiroh, N.M., 2020. A comparative study of gallic acid, ellagic acid, Urolithin A, and Urolithin B with NF-κB Protein as Anti Type 2 diabetes mellitus by in silico. JSMARTech 1, 31–35. https://doi.org/10.21776/ub.jsmartech.2020.001.02.2.

Hussein, Y.T., Azeez, Y.H., 2023. DFT analysis and in silico exploration of drug-likeness, toxicity prediction, bioactivity score, and chemical reactivity properties of the urolithins. J. Biomol. Struct. Dyn. 41, 1168–1177. https://doi.org/10.1080/07391102.2021.2017350.

Ishimoto, H., Shibata, M., Myojin, Y., Ito, H., Sugimoto, Y., Tai, A., Hatano, T., 2011. In vivo anti-inflammatory and antioxidant properties of ellagitannin metabolite urolithin A. Bioorg. Med. Chem. Lett. 21, 5901–5904. https://doi.org/10.1016/j.bmcl.2011.07.086.

Jeengar, M.K., Thummuri, D., Magnusson, M., Naidu, V.G.M., Uppugunduri, S., 2017. Uridine Ameliorates Dextran Sulfate Sodium (DSS)-Induced Colitis in Mice. Sci. Rep. 7, 3924. https://doi.org/10.1038/s41598-017-04041-9.

Jing, T., Liao, J., Shen, K., Chen, X., Xu, Z., Tian, W., Wang, Y., Jin, B., Pan, H., 2019. Protective effect of urolithin a on cisplatin-induced nephrotoxicity in mice via modulation of inflammation and oxidative stress. Food Chem. Toxicol. 129, 108–114. https://doi.org/10.1016/j.fct.2019.04.031.

Kang, I., Buckner, T., Shay, N.F., Gu, L., Chung, S., 2016. Improvements in metabolic health with consumption of ellagic acid and subsequent conversion into urolithins: evidence and mechanisms. Adv. Nutr. 7, 961–972. https://doi.org/10.3945/an.116.012575.

Karim, S., Madani, B., Burzangi, A.S., Alsieni, M., Bazuhair, M.A., Jamal, M., Daghistani, H., Barasheed, M.O., Alkreathy, H., Khan, M.A., Khan, L.M., 2023. Urolithin A's antioxidative, anti-inflammatory, and antiapoptotic activities mitigate doxorubicin-induced liver injury in wistar rats. Biomedicines 11, 1125. https://doi.org/10.3390/biomedicines11041125.

Karwasra, R., Kalra, P., Gupta, Y.K., Saini, D., Kumar, A., Singh, S., 2016. Antioxidant and anti-inflammatory potential of pomegranate rind extract to ameliorate cisplatin-induced acute kidney injury. Food Funct. 7, 3091–3101. https://doi.org/10.1039/C6FO00188B.

Kondreddy, V.K.R., Kamatham, A.N., 2016. Celecoxib, a COX-2 inhibitor, synergistically potentiates the anti-inflammatory activity of docosahexaenoic acid in macrophage cell line. Immunopharmacol. Immunotoxicol. 38, 153–161. https://doi.org/10.3109/08923973.2016.1147578.

Labib, M.B., Sharkawi, S.M.Z., El-Daly, M., 2018. Design, synthesis of novel isoindoline hybrids as COX-2 inhibitors: Anti-inflammatory, analgesic activities and docking study. Bioorg. Chem. 80, 70–80. https://doi.org/10.1016/j.bioorg.2018.05.018.

Lagunin, A., Stepanchikova, A., Filimonov, D., Poroikov, V., 2000. PASS: prediction of activity spectra for biologically active substances. Bioinformatics 16, 747–748. https://doi.org/10.1093/bioinformatics/16.8.747.

Lee, G., Park, J.-S., Lee, E.-J., Ahn, J.-H., Kim, H.-S., 2019. Anti-inflammatory and antioxidant mechanisms of urolithin B in activated microglia. Phytomedicine 55, 50–57. https://doi.org/10.1016/j.phymed.2018.06.032.

Lokhande, K.B., Doiphode, S., Vyas, R., Swamy, K.V., 2021. Molecular docking and simulation studies on SARS-CoV-2 M pro reveals Mitoxantrone, Leucovorin, Birinapant, and Dynasore as potent drugs against COVID-19. J. Biomol. Struct. Dyn. 39, 7294–7305. https://doi.org/10.1080/07391102.2020.1805019.

Lokhande, K.B., Ghosh, P., Nagar, S., Venkateswara Swamy, K., 2022. Novel B, C-ring truncated deguelin derivatives reveals as potential inhibitors of cyclin D1 and cyclin E using molecular docking and molecular dynamic simulation. Mol. Divers. 26, 2295–2309. https://doi.org/10.1007/s11030-021-10334-z.

Lokhande, K.B., Shrivastava, A., Singh, A., 2023. In silico discovery of potent inhibitors against monkeypox's major structural proteins. J. Biomol. Struct. Dyn. 1–16. https://doi.org/10.1080/07391102.2023.2183342.

Mi, H., Liu, S., Hai, Y., Yang, G., Lu, J., He, F., Zhao, Y., Xia, M., Hou, X., Fang, Y., 2022. Lactococcus garvieae FUA009, a novel intestinal bacterium capable of producing the bioactive metabolite Urolithin A from ellagic acid. Foods 11, 2621. https://doi.org/10.3390/foods11172621.

Mitchell, J.A., Kirkby, N.S., 2019. Eicosanoids, prostacyclin and cyclooxygenase in the cardiovascular system. Br. J. Pharmacol. 176, 1038–1050. https://doi.org/10.1111/bph.14167.

Mohammadi, M., Nejatollahi, F., Sakhteman, A., Zarei, N., 2016. Insilico analysis of three different tag polypeptides with dual roles in scFv antibodies. J. Theor. Biol. 402, 100–106. https://doi.org/10.1016/j.jtbi.2016.04.016.

More-Adate, P., Lokhande, K.B., Swamy, K.V., Nagar, S., Baheti, A., 2022. GC-MS profiling of Bauhinia variegata major phytoconstituents with computational identification of potential lead inhibitors of SARS-CoV-2 Mpro. Comput. Biol. Med. 147,. https://doi.org/10.1016/j.compbiomed.2022.105679 105679.

Morris, G.M., Lim-Wilby, M., 2008. Molecular Docking. pp. 365–382. Doi: 10.1007/978-1-59745-177-2_19.

Nascimento, S., Duarte, C., Araruna, S., 2016. Phytochemicals of PunicaGranatum L. in inflammatory bowel diseases: an update. Sci. Forum 2 (14), 1–5.

Nesaragi, A.R., Kamble, R.R., Dixit, S., Kodasi, B., Hoolageri, S.R., Bayannavar, P.K., Dasappa, J.P., Vootla, S., Joshi, S.D., Kumbar, V.M., 2021. Green synthesis of therapeutically active 1,3,4-oxadiazoles as antioxidants, selective COX-2 inhibitors and their in silico studies. Bioorg. Med. Chem. Lett. 43,. https://doi.org/10.1016/j.bmcl.2021.128112 128112.

Noshadi, B., Ercetin, T., Luise, C., Yuksel, M.Y., Sippl, W., Sahin, M.F., Gazi, M., Gulcan, H.O., 2020. Synthesis, characterization, molecular docking, and biological activities of some natural and synthetic urolithin analogs. Chem. Biodivers. 17. https://doi.org/10.1002/cbdv.202000197.

Orlando, B.J., Malkowski, M.G., 2016. Crystal structure of rofecoxib bound to human cyclooxygenase-2. Acta Crystallogr. Sect. F Struct. Biol. Commun. 72, 772–776. https://doi.org/10.1107/S2053230X16014230.

Rana, S., Dixit, S., Mittal, A., 2019. In silico target identification and validation for antioxidant and anti-inflammatory activity of selective phytochemicals. Brazilian Arch. Biol. Technol. 62. https://doi.org/10.1590/1678-4324-2019190048.

Rasheed, U., Ilyas, U., Zaman, S.U., Muhammad, S.A., Afzaal, H., Altaf, R., 2018. ADME/T prediction, molecular docking, and biological screening of 1,2,4-Triazoles as potential antifungal agents. J. Appl. Bioinforma. Comput. Biol. 07. https://doi.org/10.4172/2329-9533.1000144.

Refaey, M., Abouelela, M., El-Shoura, E., Alkhalidi, H., Fadil, S., Elhady, S., Abdelhameed, R., 2022. In vitro anti-inflammatory activity of cotula anthemoides essential oil and in silico molecular docking of its bioactives. Molecules 27, 1994. https://doi.org/10.3390/molecules27061994.

Rouzer, C.A., Marnett, L.J., 2020. Structural and chemical biology of the interaction of cyclooxygenase with substrates and non-steroidal anti-inflammatory drugs. Chem. Rev. 120, 7592–7641. https://doi.org/10.1021/acs.chemrev.0c00215.

Shah, K., Mujwar, S., Gupta, J.K., Shrivastava, S.K., Mishra, P., 2019. Molecular docking and in silico cogitation validate mefenamic acid prodrugs as human Cyclooxygenase-2 inhibitor. Assay Drug Dev. Technol. 17, 285–291. https://doi.org/10.1089/adt.2019.943.

Shahraki, A., Ebrahimi, A., 2019. Binding of ellagic acid and urolithin metabolites to the CK2 protein, based on the ONIOM method and molecular docking calculations. New J. Chem. 43, 15983–15998. https://doi.org/10.1039/C9NJ03508G.

Sharma, A.D., Kaur, I., Singh, N., 2021. Tryptophan fluorescence spectroscopy: key tool to study protein denaturation/anti-inflammatory assay. Res. Rev. Biotechnol. Biosci. 8. https://doi.org/10.5281/zenodo.5118388.

Shukla, M., Gupta, K., Rasheed, Z., Khan, K.A., Haqqi, T.M., 2008. Bioavailable constituents/metabolites of pomegranate (Punica granatum L) preferentially inhibit COX2 activity ex vivo and IL-1beta-induced PGE2 production in human chondrocytes i n vitro. J. Inflamm. 5, 9. https://doi.org/10.1186/1476-9255-5-9.

Smith, W.L., DeWitt, D.L., Garavito, R.M., 2000. Cyclooxygenases: structural, cellular, and molecular biology. Annu. Rev. Biochem 69, 145–182. https://doi.org/10.1146/annurev.biochem.69.1.145.

Suručić, R., Travar, M., Petković, M., Tubić, B., Stojiljković, M.P., Grabež, M., Šavikin, K., Zdunić, G., Škrbić, R., 2021. Pomegranate peel extract polyphenols attenuate the SARS-CoV-2 S-glycoprotein binding ability to ACE2 Receptor: in silico and in vitro studies. Bioorg. Chem. 114,. https://doi.org/10.1016/j.bioorg.2021.105145 105145.

Taidi, L., Maurady, A., Britel, M.R., 2022. Molecular docking study and molecular dynamic simulation of human cyclooxygenase-2 (COX-2) with selected eutypoids. J. Biomol. Struct. Dyn. 40, 1189–1204. https://doi.org/10.1080/07391102.2020.1823884.

ul Hassan, S.S., Zhang, W.-D., Jin, H., Basha, S.H., Priya, S.V.S.S., 2022. In-silico anti-inflammatory potential of guaiane dimers from Xylopia vielana targeting COX-2. J. Biomol. Struct. Dyn. 40, 484–498. https://doi.org/10.1080/07391102.2020.1815579.

Williams, C.S., Mann, M., DuBois, R.N., 1999. The role of cyclooxygenases in inflammation, cancer, and development. Oncogene 18, 7908–7916. https://doi.org/10.1038/sj.onc.1203286.

Yaraguppi, D.A., Deshpande, S.H., Bagewadi, Z.K., Kumar, S., Muddapur, U.M., 2021. Genome analysis of Bacillus aryabhattai to identify biosynthetic gene clusters and in silico methods to elucidate its antimicrobial nature. Int. J. Pept. Res. Ther. 27, 1331–1342. https://doi.org/10.1007/s10989-021-10171-6.

Yaraguppi, D.A., Bagewadi, Z.K., Deshpande, S.H., Chandramohan, V., 2022. In silico study on the inhibition of UDP-N-Acetylglucosamine 1-Carboxy Vinyl transferase from salmonella typhimurium by the lipopeptide produced from Bacillus aryabhattai. Int. J. Pept. Res. Ther. 28, 80. https://doi.org/10.1007/s10989-022-10388-z.

Zhang, M., Cui, S., Mao, B., Zhang, Q., Zhao, J., Zhang, H., Tang, X., Chen, W., 2022. Ellagic acid and intestinal microflora metabolite Urolithin A: a review on its sources, metabolic distribution, health benefits, and biotransformation. Crit. Rev. Food Sci. Nutr. 1–23. https://doi.org/10.1080/10408398.2022.2036693.